Technical Memorandum No. 97
Addendum to ECOM Report
03733-F

# Step-Tunable VHF Power Amplifier

By
N. E. Abbott
R. C. Rehner

For

U. S. ARMY ELECTRONICS COMMAND
FORT MONMOUTH, NEW JERSEY

COOLEY ELECTRONICS LABORATORY
Department of Electrical Engineering
The University of Michigan

Contract No. DA-36-039 AMC-03733(E)
Signal Corps, Department of the Army
Department of the Army Project No. 1G0 21101 A04201

February 1966

Technical Memorandum No. 97

# STEP-TUNABLE VHF POWER AMPLIFIER

by


N. E. Abbott
R. C. Rehner, Jr.


Approved by: T. W. Butler, Jr.

T. W. Butler, Jr.

for


COOLEY ELECTRONICS LABORATORY

Department of Electrical Engineering
The University of Michigan
Ann Arbor, Michigan



Contract No. DA-36-039 AMC-03733(E)
Signal Corps, Department of the Army
Department of the Army Project No. 1G0 21101 A04201


February 1966

## TABLE OF CONTENTS

## LIST OF ILLUSTRATIONS

## ABSTRACT

The characteristics of a VHF power amplifier that is to be electronically tuned in the VHF band are theoretically and experimentally analyzed. This tuning method involves varying the electrical length of a transmission line by electronically short circuiting the line at different positions. PIN diodes are selected to perform this short circuiting function.

The optimum characteristic impedance of the transmission line and the location of the PIN diodes along the line are determined with the aid of a computer.

This memorandum also discusses problems of multiple resonance frequencies and bandwidth reduction. Experimental measurements of diode locations, multiple resonance frequencies, and bandwidth substantiate the theoretical considerations.

Finally, a proposed configuration for fabricating the amplifier is presented.

## I. INTRODUCTION

This memorandum discusses design considerations for the development of an electronically tunable VHF power amplifier. The basic design objectives are:

(1) Output power - 100 watts

(2) Tuning range - 60 Mc to 300 Mc

(3) Instantaneous bandwidth - 10 Mc to 20 Mc

(4) Tuning rate (from one center frequency to another center frequency) - 5 to 10 $\mu$sec

(5) Overlap between adjacent bands - 0.5 Mc to 2 Mc

(6) Load impedance - 50Ω nominal with maximum VSWR of 3

(7) Plate circuit efficiency - 30 percent to 40 percent

Power amplifiers covering this VHF frequency range have been developed which utilize distributed amplifier techniques. However, such distributed amplifiers generally possess low plate circuit efficiencies. A narrow bandwidth Class C amplifier is capable of providing improved efficiency characteristics. Thus, it is desirable to develop a method for rapidly tuning a narrowband power amplifier across the VHF band. Such a scheme should be able to provide effective wideband coverage without the sacrifice of efficiency.

A relatively straightforward scheme for rapid tuning is selected to simplify the analysis. Considerations of similar but more complex tuning methods can be made once the characteristics of the basic tuning problem are determined.

## 2. PRELIMINARY CONSIDERATIONS

The configuration under consideration is shown in Fig. 1. A common cathode gain stage utilizing a 4X250B power tetrode was selected to provide the necessary gain, output power, and frequency range (Ref. 1). The voltage and current requirements of the transmission line shorting switches are of primary importance. An approximate determination of these switch requirements is given in the Appendix. A switch in the "open" position must be able to withstand peak potentials of about 1000 volts. A switch in the "closed" position will have to conduct RF currents on the order of 7 amperes RMS.

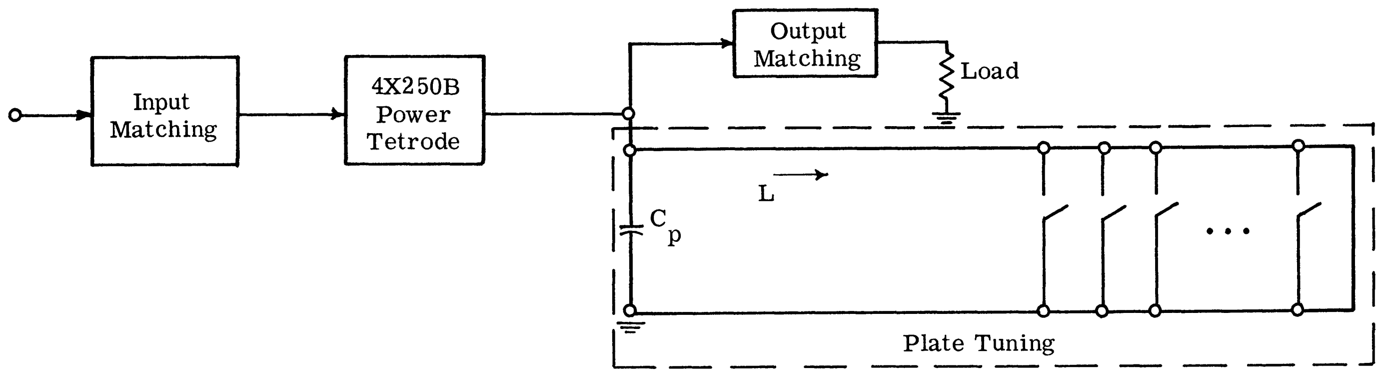


Where L is a variable inductance produced by a single short circuited transmission line with step-variable length.

Fig. 1. Power amplifier configuration.

## 3. SELECTION OF SWITCHING DEVICE

Several types of devices were considered for performing the switching function. These were:

(1) Reed relays

(2) Silicon controlled rectifiers

(3) High voltage transistors

(4) PIN diodes

### 3.1 Reed Relays

Reed relays can satisfy the voltage and current requirements; and, they also have very small "on" resistances. However, the switching speeds of reed relays are much too slow to satisfy the switching requirement of 5 to 10 $\mu$sec per step.

### 3.2 Silicon Controlled Rectifiers

High power silicon controlled rectifiers can also satisfy the voltage and current requirements at low frequencies. Unfortunately, they possess relatively large anode capacities and are difficult to turn off. A more fundamental limitation of SCR's in this application is a result of capacitive coupling from the anode to gate. With typical high power SCR's, the rise time of the anode potential must be limited to a maximum of about 500 volts/$\mu$sec to prevent the anode to gate capacitance from coupling sufficient current into the gate to turn the device on. The approximate rise time encountered in this application is 50,000 volts/$\mu$sec. Therefore, SCR's are not allowable.

### 3.3 High Voltage Transistors

Recent developments in the state of the art have yielded silicon transistors with collector-base breakdown voltages of several hundred volts. It would be possible to series connect two or three high voltage transistors to produce a switch capable of withstanding the 1000 volt peak potential. However, the large collector junction areas required to handle the high RF current cause large collector capacitances (100 pf to 1000 pf). In addition, the low collector doping concentrations consistent with high breakdown voltages cause increased series resistances (1Ω to 5Ω). For these reasons, transistors are not suitable in this switching application.

## 3.4 PIN Diodes

PIN diodes seem to offer the most feasible solution to the switching problem. A source of silicon PIN diodes meeting the current and voltage requirements has been found. The devices are manufactured by the Semiconductor Division of Sylvania Electric Products, Inc., and bear a special part designation D5618. Typical device characteristics are as follows:

| | |
|---|---|
| Minimum reverse breakdown voltage: | $BV_{min} \geq$ 1 kv at 10 μa |
| Maximum average forward current: | $I_{maxAvg}$ = 8 Amp |
| Typical total capacitance: | $C_p \approx$ 5 pf at -50 v, 1 Mc |
| Typical series resistance: | $R_s \approx$ 0.5Ω at 100 ma, 500 Mc |
| Maximum series inductance: | $L_{smax} \leq$ 2 nh |
| Typical junction-to-case thermal resistance: | $\theta_{J\text{-}C}$ = 8° C/W |
| Maximum operating junction temperature: | $T_{Jmax}$ = 175° C |

Three diodes of this type were tested. They exhibited breakdown voltages of 820 v, 850 v, and 980 v; average capacitances of 8.9 pf, 8.4 pf, and 8.9 pf; and series resistances of 0.41Ω, 0.45Ω, and 0.45Ω. The manufacturer has indicated that breakdown voltage and capacitance specifications can be met by selection of diodes from their existing PIN production.

## 4. DIODE CHARGE STORAGE EFFECT

Experimental measurements were also made to determine the amount of forward bias current ($I_{dd}$) necessary for maintaining diode conduction during both half cycles of the RF current ($I_{RF}$).

For example,

$$I_{diode} = I_{dd} + I_{RF} \sin \omega t$$

where

$$I_{RF} \approx 7\sqrt{2} \text{ amperes, according to the Appendix}$$

$$I_{diode} = \text{total diode current.}$$

In general, to maintain diode conduction

$$I_{diode} > 0$$

Requiring

$$I_{dd} > I_{RF}$$

Thus, the peak diode current would be

$$I_{diode\ peak} = I_{dd} + I_{RF} > 2(7\sqrt{2}) \approx 20 \text{ amperes}$$

and a PIN diode with current capability of more than 8 amperes would be required. However, at high frequencies, charge stored across the diode junction during the forward half-cycle of the RF current can contribute the carriers necessary for sustaining the current during the reverse half-cycle. This effect was measured at a frequency of 60 Mc. It was found that the charge storage effect was sufficient to sustain the reverse half-cycle RF current even without the application of the forward bias current.

The series "on" resistance of the PIN diodes is reduced by a conductivity modulation effect under the influence of forward bias current. Due to this effect, a forward bias current of about 100 ma is required to reduce the series resistance to the 0.5Ω value.

## 5. DETERMINATION OF $Z_0$ AND SWITCH LOCATIONS

Given the diode switch characteristics, it is possible to select an optimum characteristic impedance ($Z_0$) for the transmission line and to determine the switch locations along the line. The choice of $Z_0$ affects the degree to which a reverse biased diode appears as an open switch and a forward biased diode appears as a closed switch across the transmission line. The choice of $Z_0$ also affects the magnitude of the RF current flowing through a closed switch, the length of the transmission line, and the instantaneous bandwidth of the single tuned plate circuit. In all these considerations, except that of simulating the open switch condition, it is desirable to make $Z_0$ as large as possible.

A computer solution was obtained to determine the switch locations to cover the frequency band in 20 Mc steps (Figs. 2 and 3). Figure 2 is the solution for ideal switches. In Fig. 3, an "on" diode was approximated as an ideal switch with zero series resistance; and an "off" diode was approximated as a 5 pf capacitor. The output capacitance of the tube plus the stray and trimming capacitance was assumed to be 20 pf. By using $Z_0$ as a variable parameter, its effect on the diode locations can be readily seen. For the stated assumptions, $Z_0$ must be limited to a maximum of about 30Ω to prevent the diode locations from being too close physically for practical diode packages.

## 6. REASON FOR ASSUMING DEFINITE $C_T$ VALUE

If the total plate circuit capacitance is other than the assumed 20 pf value, the change in center frequency corresponding to a change in equivalent inductance will vary accordingly. The relationship between the change in center frequency resulting from a change in inductance has been found to be:

$$\Delta f_0 = -2\pi^2 f_0^3 C_T \Delta L$$

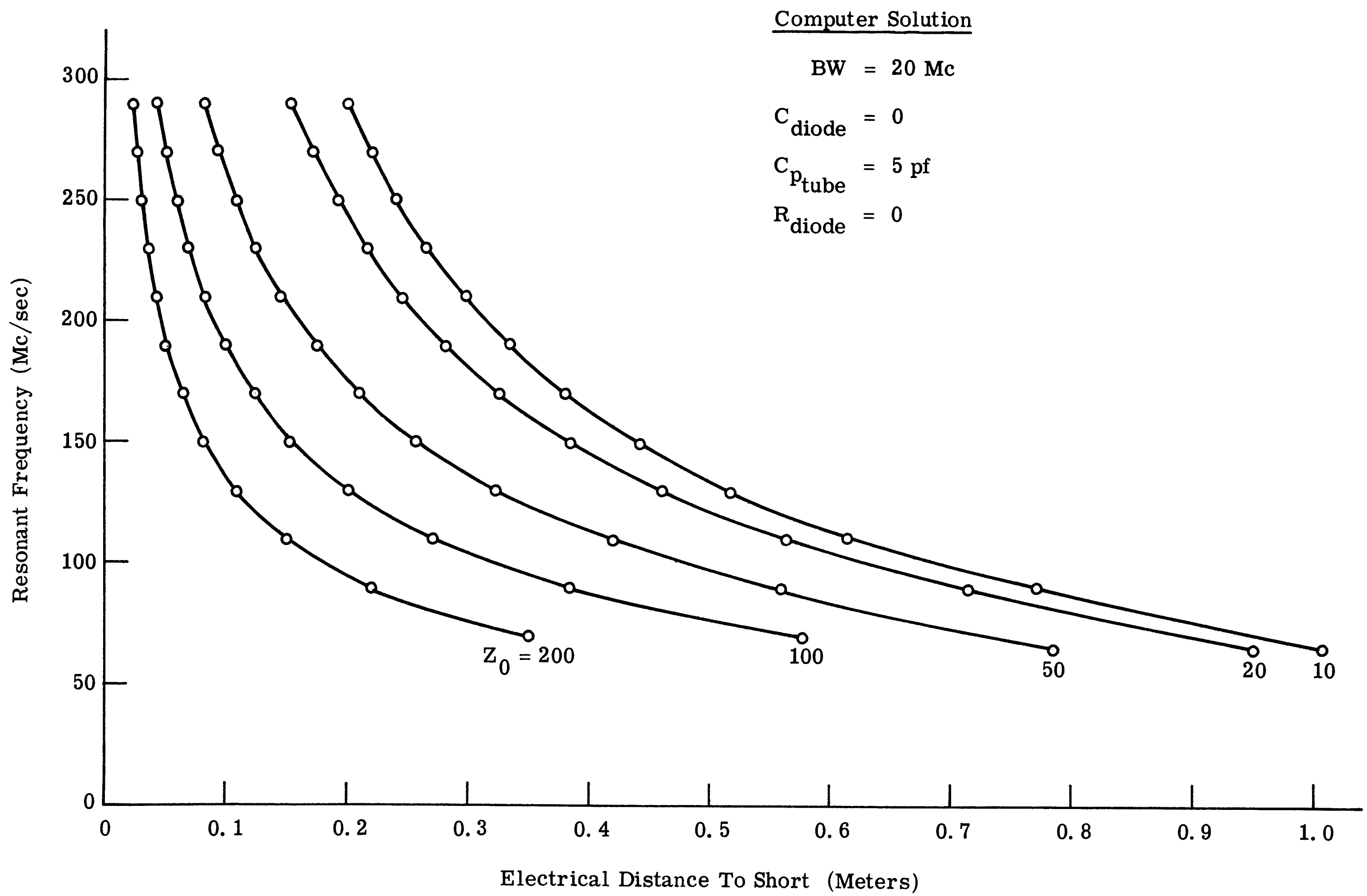


Fig. 2. Locations of ideal switches.

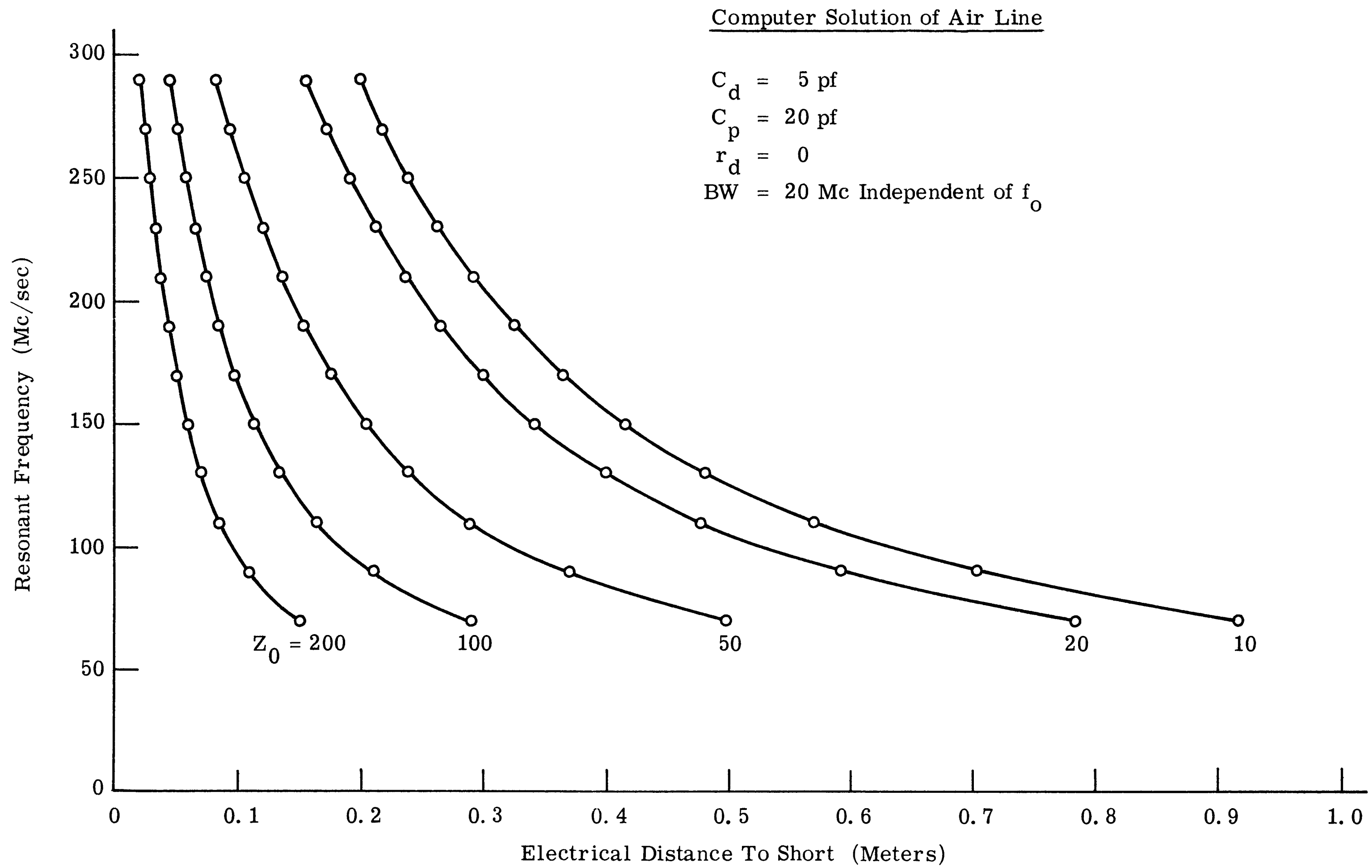


Fig. 3. Locations of switches with shunt capacitances.

where

$f_0$ = center frequency

$\Delta f_0$ = change in center frequency

$C_T$ = total plate circuit capacitance

$\Delta L$ = change in equivalent inductance

$C_T$ can be adjusted to a predetermined value with trimming capacitance so that center frequencies and changes in center frequencies correspond to calculated values.

## 7. MULTIPLE RESONANCES OF PLATE CIRCUIT

The use of a shorted transmission line to simulate an ideal inductor introduces additional problems into the design of the plate tuning. For an ideal transmission line, the plate circuit will be resonant for those frequencies at which:

$$\frac{1}{2\pi f C_T} = Z_0 \tan \frac{2\pi f}{\upsilon} x$$

In general, if this transcendental equation is satisfied at a frequency $f_0$ and the line length x is on the order of a quarter wavelength; it will be satisfied at higher frequencies approximately equal to $3f_0$, $5f_0$, $7f_0$, etc. This multiple resonance phenomena may be especially troublesome in a Class C amplifier since the plate current pulse is rich in harmonics and only the fundamental voltage component is desired. The multiple resonances of the plate circuit would allow not only the fundamental voltage component but also all odd harmonics of it. This would distort the output waveform and could reduce both the fundamental output power and the efficiency of the amplifier. Perhaps it will be desirable to provide some tuning of the output matching network to prevent the dissipation of power in the load at the harmonic frequencies.

## 8. BANDWIDTH LIMITATIONS

Another problem resulting from tuning the plate circuit with a transmission line instead of an inductor is one of reduced instantaneous bandwidths. For example, the bandwidth at a simple resonance pole is given by:

$$BW = \frac{f_0}{Q}$$

where

$$f_0 = \frac{\omega_0}{2\pi} = \text{resonance frequency}$$

$$Q = \frac{1}{2}\,\omega_0 Z_{\omega_0}\,\frac{dB}{d\omega}\bigg|_{\omega_0} \qquad \text{(Ref. 2)}$$

$$Z_{\omega_0} = Z(\omega)\Big|_{\omega = \omega_0} = \text{network impedance at resonance}$$

$$B = \text{total network susceptance}$$

$$\frac{dB}{d\omega}\bigg|_{\omega_0} = \frac{dB}{d\omega}\bigg|_{\omega = \omega_0} = \text{slope of network susceptance at resonance}$$

For the network shown in Fig. 4, the total susceptance is given by:

$$B = \omega C - \frac{1}{\omega L}$$

Also at resonance $\omega_0$: $L = \dfrac{1}{\omega_0^{\,2} C}$, $Z_{\omega_0} = R$

From these relationships the resulting bandwidth is determined to be:

$$BW = \frac{1}{2\pi RC}$$

Now if the inductor is replaced with a lossless short circuited transmission line (Fig. 5), the expression for total network susceptance is changed.

$$B = \omega C - \frac{1}{Z_0} \cot \frac{\omega}{\upsilon}\, x$$

where

$Z_0$ = characteristic impedance of transmission line

$x$ = physical length of transmission line

$\upsilon$ = velocity of propagation in transmission line

Now for resonance at $\omega_0$, we require:

$$\omega_0 C = \frac{1}{Z_0} \cot \frac{\omega_0}{\upsilon} x$$

or

$$\cot \frac{\omega_0}{\upsilon} x = Z_0 \omega_0 C$$

The expression for $\frac{dB}{d\omega}$ becomes

$$\frac{dB}{d\omega}\bigg|_{\omega_0} = C + \frac{x}{\upsilon Z_0} \csc^2 \frac{\omega_0}{\upsilon} x$$

and since

$$\csc^2 \frac{\omega_0}{\upsilon} x = 1 + \cot^2 \frac{\omega_0}{\upsilon} x$$

we can write

$$\frac{dB}{d\omega}\bigg|_{\omega_0} = C + \frac{x}{\upsilon Z_0} [1 + (Z_0 \omega_0 C)^2]$$

Thus, for the case of transmission line tuning, the bandwidth may be expressed as:

$$BW = \frac{1/\pi}{RC + \frac{Rx}{\upsilon Z_0} [1 + (Z_0 C \omega_0)^2]}$$

The above expression indicates that the bandwidth is not limited simply by the RC product as it was in the case involving the inductor tuning. In fact, in the range of interest, the denominator term $\frac{Rx}{\upsilon Z_0}$ is larger than the RC term. As a result, bandwidths associated with transmission line tuning will be narrower than those associated with inductor tuning.

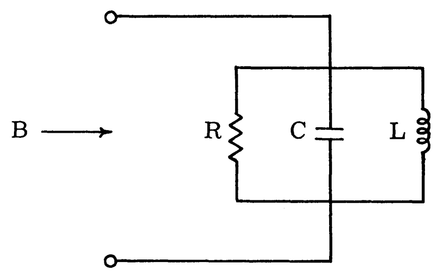


Fig. 4. Inductor tuning.

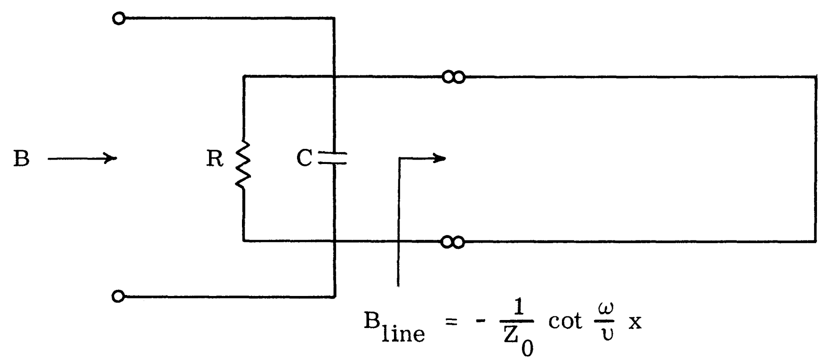


Fig. 5. Transmission line tuning.

## 9. EXPERIMENTAL TRANSMISSION LINE TUNING

To verify the computer solution for the switch locations along the transmission line, and to study the multiple resonance effect and bandwidth limitation effect; an experimental stripline was constructed. In consideration of the computer solutions, an arbitrary characteristic impedance of 10Ω was selected.

The transmission line for the experimental measurements was constructed in the form of a parallel plane stripline (Fig. 6). The $Z_0$ of such a parallel plane transmission line is given by

$$Z_0 = \frac{h}{w} \; \frac{\mu}{\epsilon}^{\frac{1}{2}}, \qquad h << w$$

where

w = width of narrower plane

h = distance between planes

The experimental line was constructed using two planes, one 9" wide and the other 10" wide, with $\frac{1}{4}$" air spacing between the planes. The line, with these dimensions, had a $Z_0$ of about 10Ω. After determining the physical size of the line, a convenient method for approximating the PIN diodes was selected.

As was previously mentioned, the manufacturer's specifications indicate that the diodes have total reverse bias capacity of 5 pf and a forward bias series resistance of about 0. 5Ω. These characteristics were simulated by using a switched parallel RC network as illustrated in Fig. 7.

Measurements for reverse bias conditions were conducted with 5 pf capacitors connected between the top and bottom planes of the stripline. The capacitors, used to simulate the diode reverse biased conditions, were constructed using $\frac{5}{16}$ inch diameter brass rods and 0. 0075 inch thick teflon sheets. The brass rods were mounted on the upper

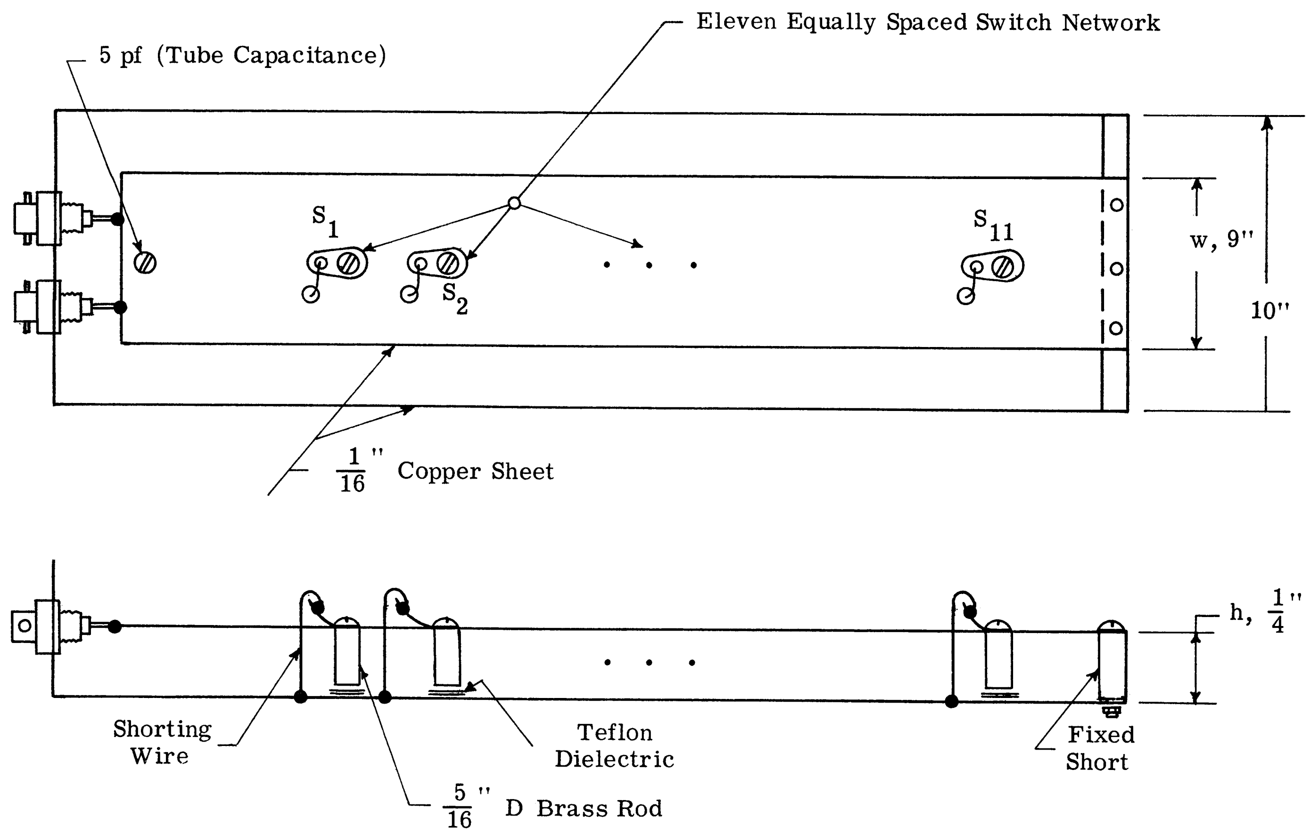


Fig. 6. Experimental transmission line.

plane and separated from the lower plane by the teflon sheets. This structure yielded capacitances of 4.6 pf across the transmission line.

The 0.5Ω resistance required for simulating a forward biased diode was difficult to obtain with high frequency resistors. For that reason, the series resistance was omitted and a forward biased diode was simulated by short circuiting the transmission line planes with a wire. These shorting wires were placed in the center of the line, alongside of their corresponding capacitors. The wires were soldered directly to the lower plane; extended through the upper plane; and then, soldered to lugs on the outside surface of the upper plane (Fig. 6). Preliminary measurements indicated that such a single wire in the center of a wide transmission line did not produce an adequate short. Therefore, the shorting wires were replaced with shorting bars that could be extended across the entire width of the transmission line. Hence, the shorting bar method was used in obtaining the experimental data. In the actual stripline, it will be important to reduce the line width so that a diode will produce an adequate RF short.

Eleven of these diode equivalent networks were placed at equal intervals along the line so that the longest and shortest line lengths would resonate the assumed tube output capacity of 5 pf at 70 Mc and 290 Mc, respectively. Measurements were made to determine the resonance frequencies and the bandwidths as a function of the simulated "on" diode positions. The experimental measurement method is shown in Fig. 8. The results of these measurements are shown in Figs. 9, 10, 11, and 12.

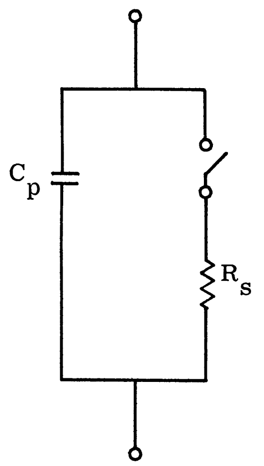


Fig. 7. Experimental PIN diode equivalent.

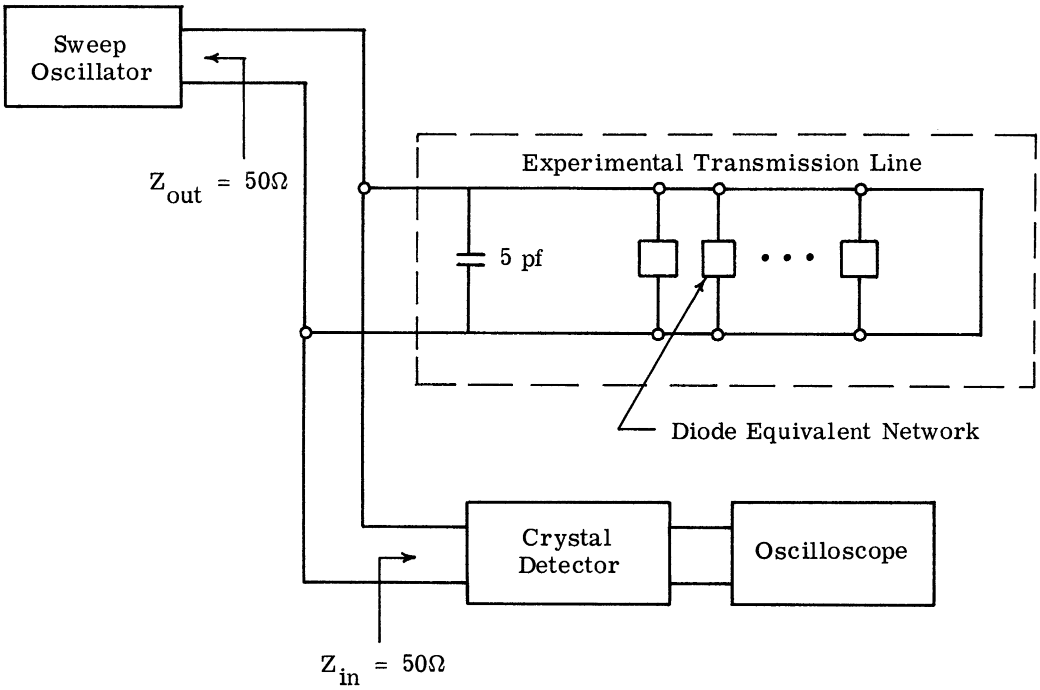


Fig. 8. Measurement circuit for experimental transmission line.

## 10. DISCUSSION OF EXPERIMENTAL RESULTS

The experimental results in Figs. 9 and 10 are for the 10Ω transmission line with equivalent diode capacitances (5 pf) placed at the location of each switch. Figures 11 and 12 are corresponding results for the case with no equivalent diode shunt capacitances being placed down the line (i. e. , ideal diode case). Comparison of the two sets of curves indicates that the effect of the 5 pf shunt capacitance at each switch location was negligible for this case of 10Ω characteristic impedance.

Figure 9 illustrates the multiple resonances resulting from the periodic nature of the transmission line. Higher harmonic modes were not measured because they were outside the frequency range of the test equipment. It should be noted that the modes shown exhibit an approximately odd-harmonic relationship to the fundamental resonance curve.

As discussed previously, the bandwidths shown in Fig. 10 are narrower than predicted by the simple relationship:

$$BW = \frac{1}{2\pi RC_T}$$

For example, consider the bandwidth measured for the fundamental resonance curve at a center frequency of 290 Mc. The equivalent resistance (R = 25Ω) and the equivalent capacitance ($C_T$ = 5 pf) predict a $\frac{1}{2\pi RC_T}$ bandwidth of 1. 28 Gc instead of the measured 124 Mc. However, if the previously developed bandwidth expression for transmission line tuning is applied:

$$BW = \frac{1/\pi}{RC + \frac{Rx}{\upsilon Z_0}\left[1 + (Z_0 C\omega_0)^2\right]}$$

where

$$R = 25\Omega$$

$$C = 5 \text{ pf}$$

$$x = 0.239 \text{ meter}$$

$$\upsilon = 3 \times 10^8 \text{ meter/sec}$$

$$Z_0 = 10\Omega$$

$$\omega_0 = 2\pi(290 \text{ Mc}) = 1.82 \times 10^9 \text{ rad/sec}$$

Then a bandwidth of 138 Mc is predicted. This predicted bandwidth agrees reasonably well with the experimentally measured bandwidth of 124 Mc.

The experimental curve of Fig. 10 also indicates an approximate four-to-one instantaneous bandwidth variation as the center frequency is tuned across the desired band. This information can be used to improve the assumption of a constant 20 Mc bandwidth which was used in the original computer solutions.

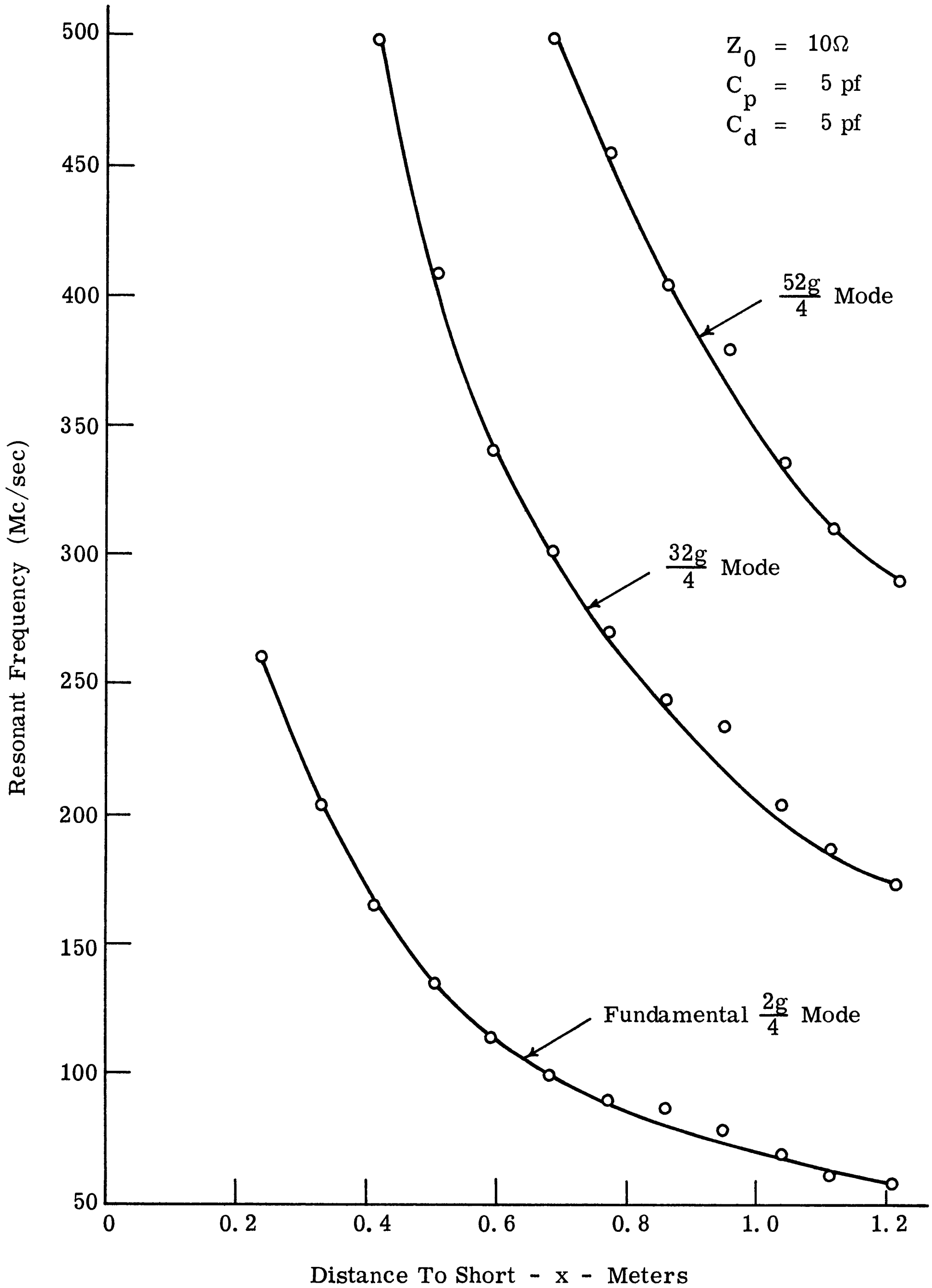


Fig. 9. Experimental transmission line resonance frequencies.

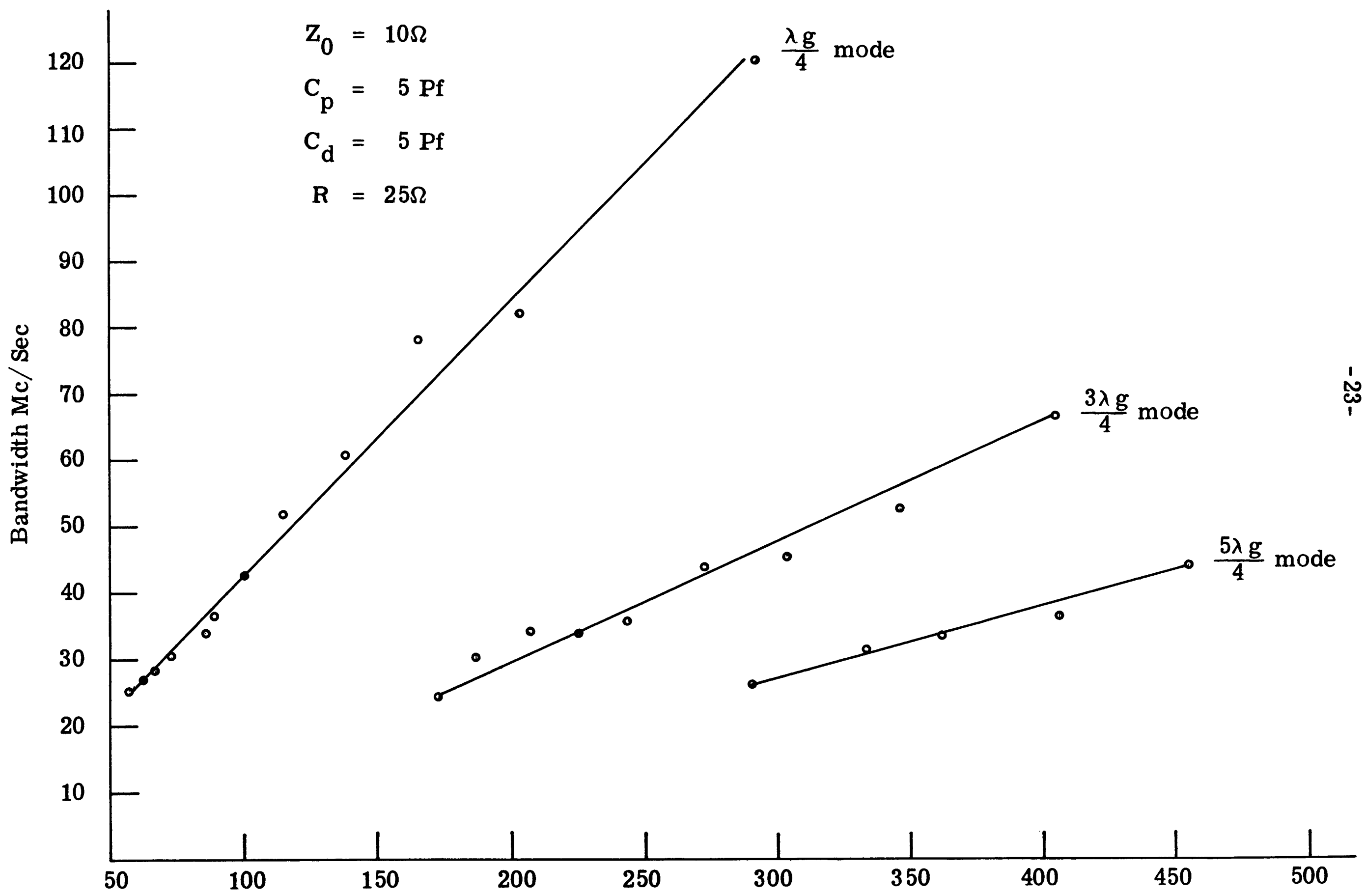


Fig. 10. Experimental Transmission Line Bandwidth Versus Resonant Frequency

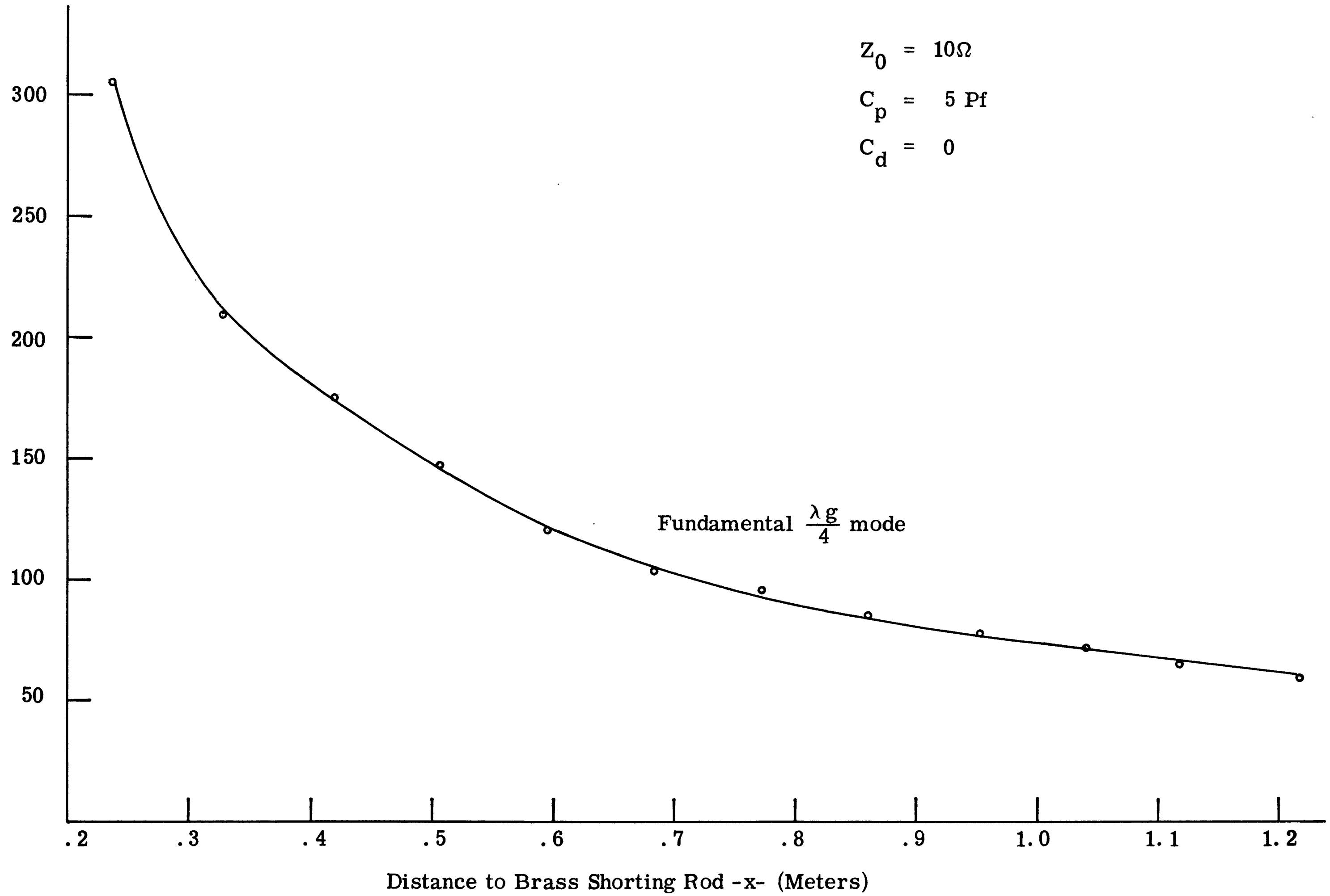


Fig. 11. Experimental Transmission Line Fundamental Resonant Frequency

## 11. PROPOSED AMPLIFIER CONFIGURATION

The configuration proposed, at present, for realizing the wideband amplifier is shown in Fig. 13. The transmission line will be realized in enclosed stripline form. The diodes will be embedded in the stripline and biased via feed through capacitors as illustrated in Fig. 14.

The use of a dielectric filled stripline with a center conductor enclosed between two ground planes allows the width of the center conductor to be reduced while maintaining a low characteristic line impedance. As a typical example, a 20Ω characteristic impedance can be realized with a center conductor width of 0. 6 inch if the distance between ground planes is 0. 25 inch and the relative dielectric constant is about 2. 3. Thus, effective RF shorts should be produced by diodes placed along the 0. 6 inch center conductor.

The plate voltage supply may be introduced through the center conductor of the stripline, thus, eliminating the need for an RF choke at the plate. This also eliminates the self resonance problems of such a choke. The current source is necessary for supplying the 100 ma forward bias to the "on" PIN diode and $E_{dd}$ will be on the order of 5 volts. Hence, the diode bias power required will be approximately one-half watt. The electronic circuitry for performing the switching logic and driver section has not been developed and will be considered only after most other details of the amplifier have been determined. The input and output matching networks have not been developed, but it is anticipated that they will employ wideband transformers realized in the form of strip-transmission lines.

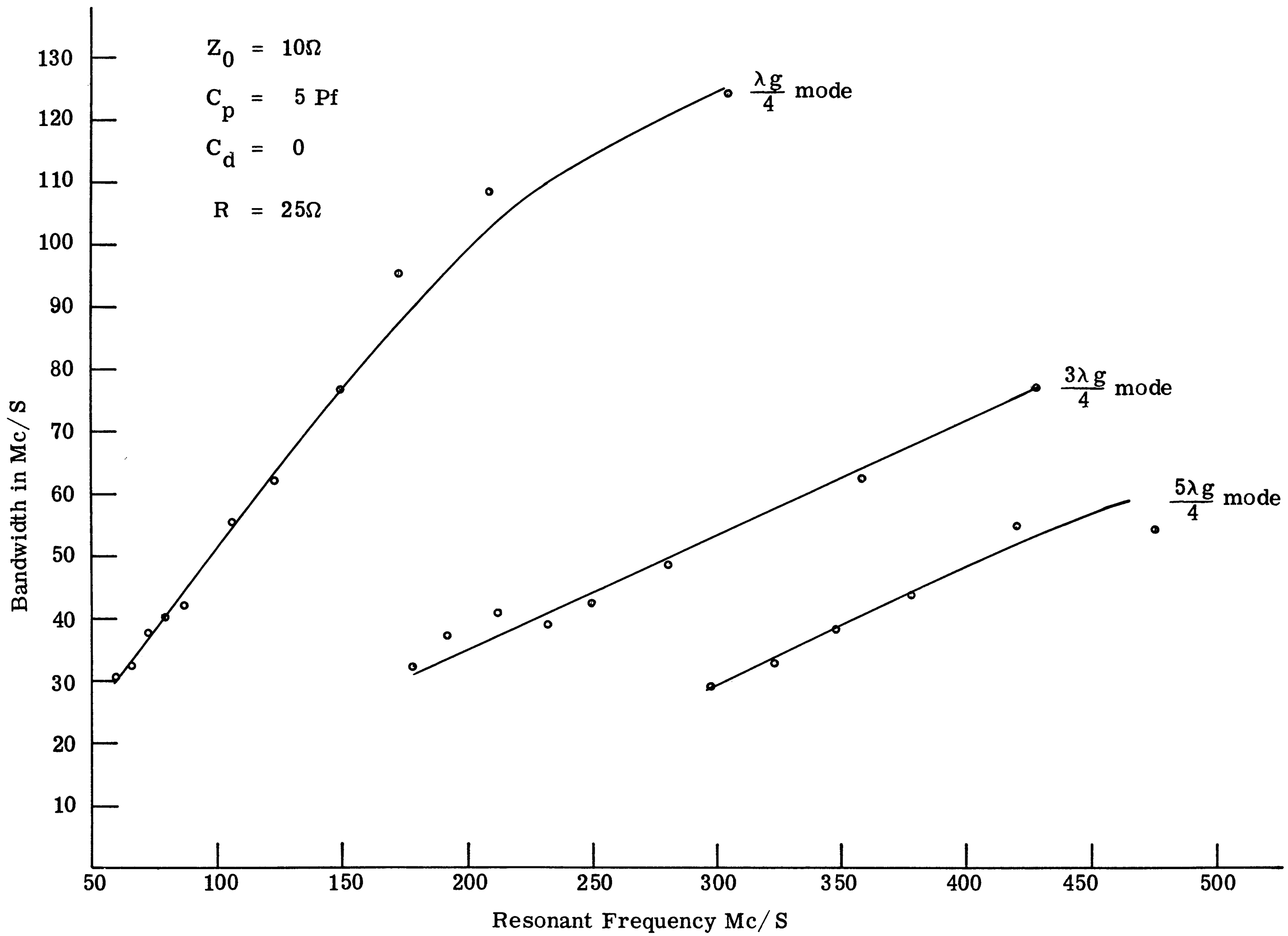


Fig. 12. Experimental Transmission Line Bandwidth Versus Resonant Frequency

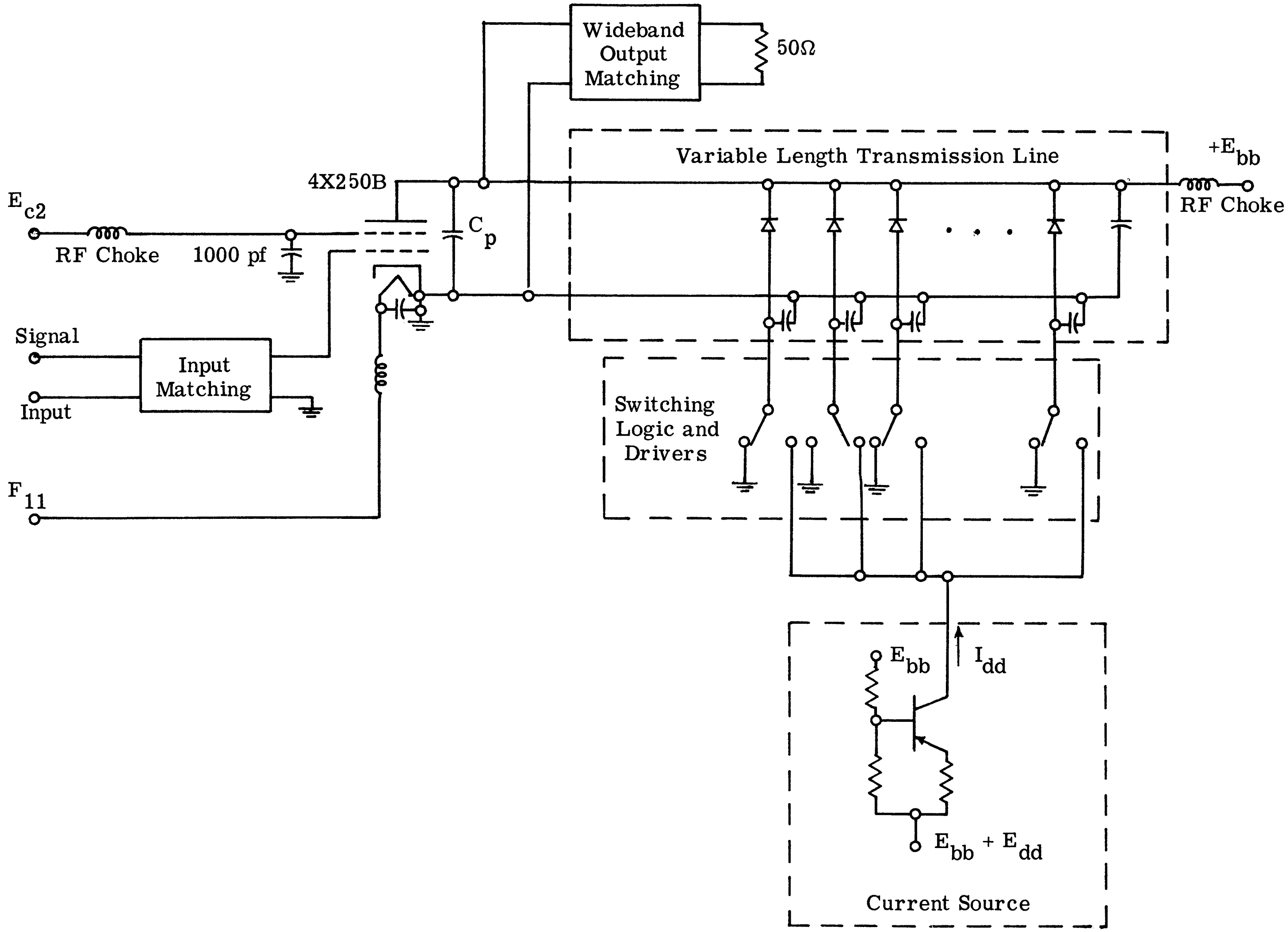


Fig. 13. Proposed amplifier configuration.

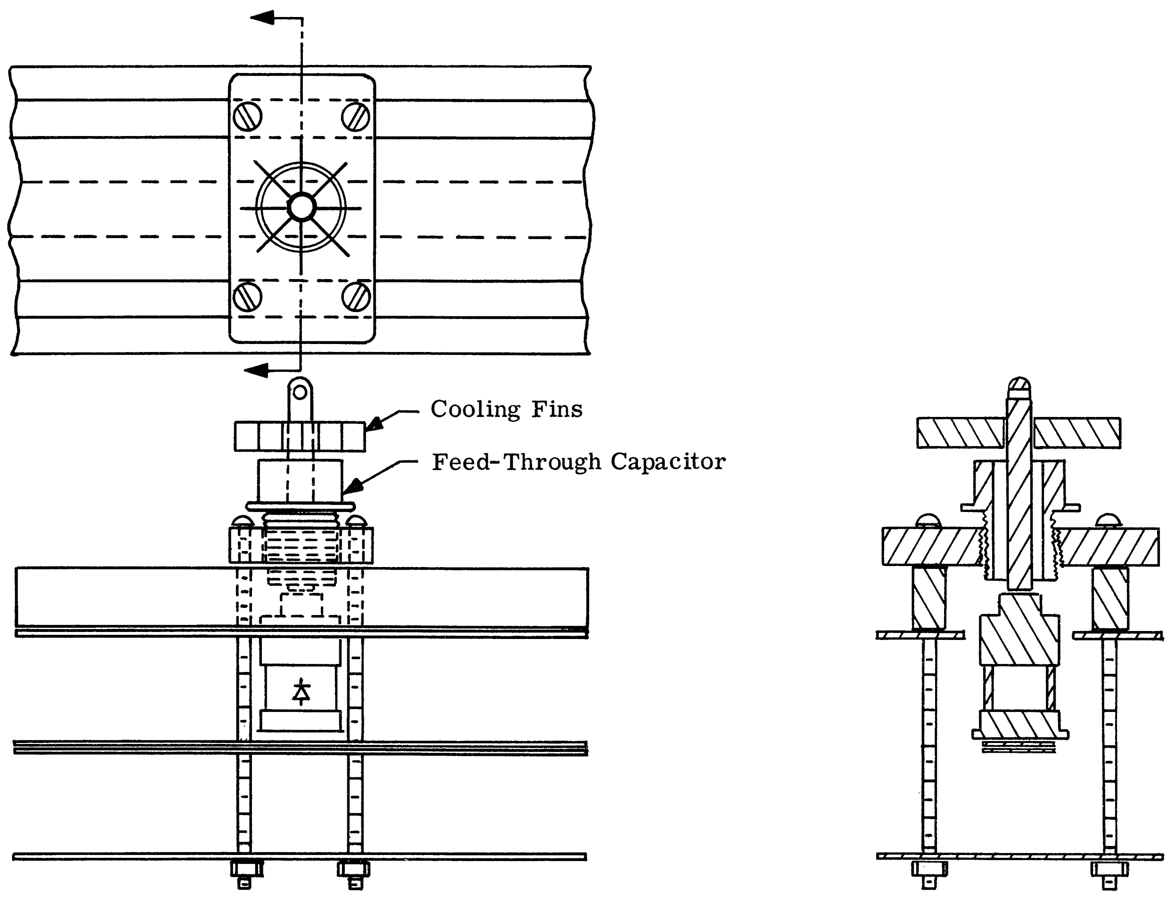

Fig. 14. Proposed diode mounting.

APPENDIX

ESTIMATE OF THE SHORTING SWITCH REQUIREMENTS

For "off" voltage requirements consider the following circuit:

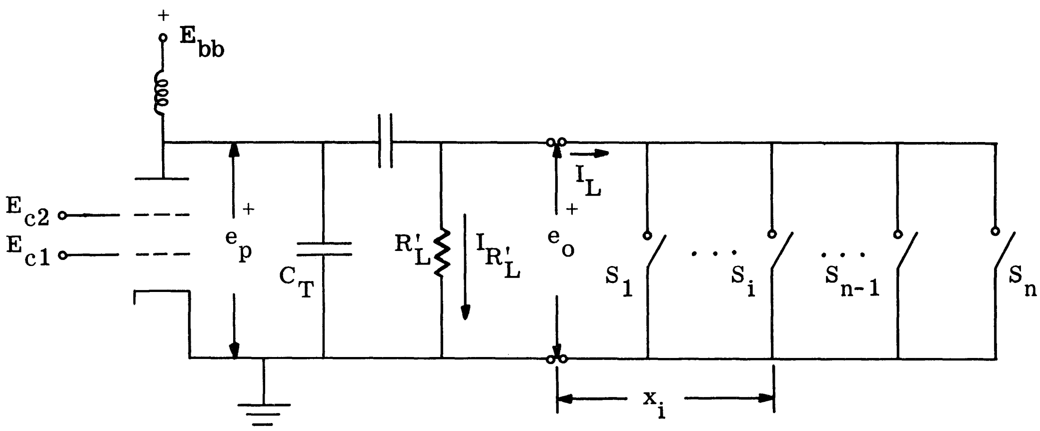


For Class C operation neglecting harmonics:

$$e_p \approx E_{bb} + (E_{bb} - E_{c2}) \sin \omega_0 t$$

Typical design values for a 4X250B tube are:

$$E_{bb} = 750 \text{ v}$$

$$E_{c2} = 250 \text{ v}$$

Giving

$$e_p = 750 + 500 \sin \omega_0 t$$

For the case of $S_1$ through $S_{n-1}$ being open and $S_n$ closed (lowest frequency):

$$e_o = 500 \sin \omega_0 t$$

and the voltage across $S_i$ is:

$$e_{si} = \frac{e_o}{\cos \frac{\pi}{2} - \frac{\omega x_n}{\upsilon}} \cos \frac{\omega}{\upsilon}(x_i - x_n) + \frac{\pi}{2}$$

The voltage across switch $S_1$ is approximately:

$$e_{s1} \approx e_o \cos \frac{\omega}{\upsilon} x_1 \leq e_o$$

Thus, a peak to peak voltage swing of about 1000 volts appears across $S_1$. Also $e_{s1} > e_{s2} > \ldots > e_{s_{n-1}}$ and $S_1$ has the most severe voltage requirement.

For the current requirements: assume

$$R_L' \approx 1\text{ K}$$

and that $C_T$ can be adjusted to give the desired bandwidth.

$$P_L' \approx \frac{e_o^2}{R_L'} = 125\text{ W}$$

$$I_{R_L'} = \frac{e_o}{R_L'} = 0.354\text{ amp RMS}$$

Now at resonance:

$$I_L = I_c = \frac{e_o}{X_c} = \frac{I_{R_L'} R_L'}{X_L} \approx Q\, I_{R_L'}$$

To determine the maximum Q to be encountered in meeting a bandwidth requirement of 20 Mc consider:

$$Q = \frac{f_o}{BW}_{max} \frac{290 \text{ Mc}}{20 \text{ Mc}} = 14.5$$

Now $I_L$ , the maximum current flowing into the terminals of the transmission line becomes:

$$I_L \approx Q \, I_{R_L}, = (14.5)(0.354) = 5.13 \text{ amp RMS}$$

The current through a shorted switch ($I_s$) at distance x from the input terminals to the line is related to the input current by the expression:

$$I_s = \frac{I_L}{\cos \frac{\omega}{\upsilon} x}$$

Now if $\frac{\omega}{\upsilon} x$ is less than $\frac{\pi}{4}$ radians

$$I_s < 1.4 \, I_L = 7.18 \text{ amp RMS}$$

## REFERENCES


1. B. F. Barton et al., Countermeasures Research, Quarterly Progress Report No. 2, Contract No. DA-36-039 AMC-03733(E), USAEMA, Cooley Electronics Laboratory, The University of Michigan, Ann Arbor, Michigan, July 1964, pp. 2-4 (SECRET).

2. D. F. Tuttle, Jr., Network Synthesis, Vol. I, Wiley, New York, 1958, p. 717.

## DISTRIBUTION LIST

| Copy No. | | Copy No. | |
|---|---|---|---|
| 1-2 | Commanding Officer<br>U.S. Army Electronics Command<br>U. S. Army Electronics Laboratories<br>Fort Monmouth, New Jersey<br>ATTN: Senior Scientist<br>Electronic Warfare Division | 11 | Headquarters<br>USAF<br>Washington 25, D. C.<br>ATTN: AFRDR |
| 3 | Commanding General<br>U. S. Army Electronic Proving Ground<br>Fort Huachuca, Arizona<br>ATTN: Director<br>Electronic Warfare Division | 12 | AFAL<br>(AVWW/ECM Technology)<br>Wright-Patterson Air Force Base<br>Ohio 45433 |
| 4 | Commanding General<br>U. S. Army Materiel Command<br>Bldg. T-7<br>Washington 25, D. C.<br>ATTN: AMCRD-DE-E | 13 | Commander<br>Aeronautical Systems Division<br>Wright-Patterson Air Force Base<br>Ohio 45433<br>ATTN: ASAPRD |
| 5 | Commanding General<br>U. S. Army Material Command<br>Bldg. T-7<br>Washington 25, D. C.<br>ATTN: AMCRD-RP-E | 14 | Commander<br>Aeronautical Systems Division<br>Wright-Patterson Air Force Base<br>Ohio 45433<br>ATTN: ASNP |
| 6 | Commanding Officer<br>Signal Corps Electronics<br>Research Unit<br>9560th USASRU<br>P. O. Box 205<br>Mountain View, California | 15 | ESD (ESTI)<br>L. G. Hanscom Field<br>Bedford, Massachusetts |
| 7 | U. S. Atomic Energy Commission<br>1901 Constitution Avenue, N. W.<br>Washington 25, D. C.<br>ATTN: Chief Librarian | 16 | Commander<br>Rome Air Development Center<br>Griffiss Air Force Base<br>New York<br>ATTN: RAYLD |
| 8 | Director<br>Central Intelligence Agency<br>2430 E Street, N. W.<br>Washington 25, D. C. | 17 | Commander<br>Air Proving Ground Center<br>Eglin Air Force Base<br>Florida<br>ATTN: ADJ/Technical Report<br>Branch |
| 9 | U. S. Army Research Liaison Officer<br>MIT-Lincoln Laboratory<br>Lexington 73, Massachusetts | 18 | Chief of Naval Operations<br>EW Systems Branch<br>OP-35, Department of the Navy<br>Washington 25, D. C. |
| 10 | Commander<br>Air Force Systems Command<br>Andrews Air Force Base<br>Washington, D. C. | 19 | Chief, Bureau of Ships<br>Code 691C<br>Department of the Navy<br>Washington 25, D. C. |

DISTRIBUTION LIST (Cont.)

| Copy No. | |
|---|---|
| 20 | Commander<br>Bu Naval Weapons Code RRRE-20<br>Department of the Navy<br>Washington 25, D. C. |
| 21 | Commander<br>Naval Ordnance Test Station<br>Inyokern<br>China Lake, California<br>ATTN: Test Director - Code 20 |
| 22 | Commander<br>Naval Air Missile Test Center<br>Point Mugu, California |
| 23 | Director<br>Naval Research Laboratory<br>Countermeasures Branch<br>Code 5430<br>Washington 25, D. C. |
| 24 | Director<br>Naval Research Laboratory<br>Washington 25, D. C.<br>ATTN: Code 2021 |
| 25 | Director<br>Air University Library<br>Maxwell Air Force Base<br>Alabama<br>ATTN: CR-4987 |
| 26 | Commanding Officer-Director<br>U. S. Navy Electronics Laboratory<br>San Diego 52, California |
| 27 | Commanding Officer<br>U. S. Naval Ordnance Laboratory<br>Silver Spring 19, Maryland |
| 28-30 | Chief<br>U.S. Army Security Agency<br>Arlington Hall Station<br>Arlington 12, Virginia 22212<br>ATTN: 2 Cpys - IADEV<br>1 Copy - EW Div. IATOP |
| 31 | President<br>U. S. Army Defense Board<br>Headquarters<br>Fort Bliss, Texas |
| 32 | President<br>U. S. Army Airborne and<br>Electronics Board<br>Fort Bragg, North Carolina |
| 33 | U. S. Army Anti-Aircraft Artillery<br>and Guided Missile School<br>Fort Bliss, Texas<br>ATTN: ORL |
| 34 | Commander<br>USAF Security Service<br>San Antonio, Texas<br>ATTN: CLR |
| 35 | Chief of Naval Research<br>Department of the Navy<br>Washington 25, D. C.<br>ATTN: Code 427 |
| 36 | Commanding Officer<br>52d U. S. Army Security Agency<br>Special Operations Command<br>Fort Huachuca, Arizona |
| 37 | President<br>U. S. Army Security Agency Board<br>Arlington Hall Station<br>Arlington 12, Virginia |
| 38 | The Research Analysis Corporation<br>McLean, Virginia 22101<br>ATTN: Document Control Officer |
| 39-48 | Headquarters<br>Defense Documentation Center<br>Cameron Station<br>Alexandria, Virginia |
| 49 | Commanding Officer<br>U. S. Army Electronics Research<br>and Development Laboratory<br>Fort Monmouth, New Jersey<br>ATTN: U. S. Marine Corps Liaison<br>Office, Code: SIGRA/SL-LNR |
| 50 | Director<br>Fort Monmouth Office<br>Communications-Electronics Combat<br>Developments Agency<br>Building 410<br>Fort Monmouth, New Jersey |

DISTRIBUTION LIST (Cont.)

| Copy No. | |
|---|---|
| 51-65 | Commanding Officer<br>U. S. Army Electronics Command<br>U. S. Army Electronics Laboratories<br>Fort Monmouth, New Jersey<br>ATTN: AMSEL-RD-DR<br>AMSEL-RD-NSR<br>AMSEL-RD-SM<br>AMSEL-RD-SA<br>AMSEL-RD-SEA<br>AMSEL-RD-SEJ<br>AMSEL-RD-SES<br>AMSEL-RD-SEE<br>AMSEL-RD-ADO<br>AMSEL-RD-SR<br>AMSEL-RD-SE<br>AMSEL-RD-ADT<br>AMSEL-RD-GFR<br>AMSEL-RD-PRM<br>AMSEL-RD-RHA |
| 66 | Commanding Officer<br>U. S. Army Signal Missile Support Agency<br>White Sands Missile Range<br>White Sands, New Mexico<br>ATTN: SIGWS-MEW |
| 67 | Commanding Officer<br>U. S. Naval Air Development Center<br>Johnsville, Pennsylvania<br>ATTN: Naval Air Development Center Library |
| 68 | U.S.A.F. Project Rand<br>The Rand Corporation<br>1700 Main Street<br>Santa Monica, California |
| 69 | Stanford Electronics Laboratories<br>Stanford University<br>Stanford, California |
| 70 | Director<br>National Security Agency<br>Fort George G. Meade, Maryland<br>ATTN: RADE-1 |
| 71 | Bureau of Naval Weapons Representative<br>Lockheed Missiles and Space Company<br>P. O. Box 504<br>Sunnyvale, California |
| 72 | Dr. T. W. Butler, Jr., Director<br>Cooley Electronics Laboratory<br>The University of Michigan<br>Ann Arbor, Michigan |
| 73-83 | Cooley Electronics Laboratory<br>The University of Michigan<br>Ann Arbor, Michigan |

Above distribution is effected by Electronic Warfare Division, Surveillance Department, USAEL, Evans Area, Belmar, New Jersey. For further information contact Mr. I. O. Myers, Senior Scientist, Telephone 59-61252.